Available online at www.sciencedirect.com
SCIENCE DIRECT®
Physica B 356 (2005) 14–20
PHYSICA B
www.elsevier.com/locate/physb

Quantification of the magnetization arrangement of patterned films measured by polarized neutron reflectivity

Katharina Theis-Bröhl[a,*], Hartmut Zabel[a], Jeffrey McCord[b], Boris P. Toperverg[c,d]

[a]*Department of Physics, Ruhr-University Bochum, D-44780 Bochum, Germany*
[b]*Leibniz Institute for Solid State and Materials Research Dresden, Helmholtzstr. 20, D-01169 Dresden, Germany*
[c]*Petersburg Nuclear Physics Institute, 188300 Gatchina, St. Petersburg, Russia*
[d]*Institut Laue Langevin, B.P. 156, Grenoble 38000, France*

Abstract

A periodic magnetic stripe array has been studied with a combination of real and reciprocal space methods: Kerr microscopy and polarized neutron reflectivity. The basic features of our experimental neutron data are well reproduced by a theoretical model using the distorted Born wave approximation and providing a set of parameters quantifying the magnetization arrangement in the stripe array system. While the specular neutron reflectivity measures a mean value of the optical potential averaged over a number of structural elements within the neutron coherence length, Bragg diffraction filters out magnetic correlation effects in the system of individual magnetic units within this length scale. Off-specular diffuse scattering probes correlations of magnetization fluctuations on a scale smaller than the coherence length. This altogether gives access to a detailed understanding of the magnetization arrangement which appears to be quite complex and hardly accessible by other methods.

PACS: 1.12.Ha; 75.75.+a; 75.70.Kw

Keywords: Polarized neutron reflectometry; Magnetic properties of nanostructures; Magnetic domains; Kerr microscopy

Lateral magnetic structures are currently discussed as important features of magneto-electronic and magnetic storage devices [1]. Much interest has been raised recently in studying their domain configurations and switching behavior. Consequently, this has developed to one of the most active fields in magnetism. Various methods are used for exploring the magnetic properties of patterned films. These methods range from normal magnetometry over imaging techniques to reciprocal space methods.

*Corresponding author.
E-mail address: k.theis-broehl@rub.de (K. Theis-Bröhl).

0921-4526/$ - see front matter © 2004 Elsevier B.V. All rights reserved.
doi:10.1016/j.physb.2004.10.037

Most recently, it was demonstrated that PNR is a powerful tool for studying the magnetic properties of patterned thin films [2–6]. The lateral structure is reproduced in reciprocal space by Bragg reflections from the lateral periodicity. In addition to information gained from the specular reflectivity, diffraction and off-specular diffuse scattering provides further insight into correlation effects between magnetization of the individual periodic elements during the magnetization reversal. In particular, quantitative analysis of the Bragg and the specular reflections provides information about the distribution of the mean magnetization over the structural elements, while the evaluation of diffuse scattering allows to quantify correlation properties of the magnetization vector fluctuation on a distance smaller than the lateral coherence length. These fluctuations are due to small domains within the structural elements. Their magnetic moment directions are correlated either within the individual and between neighboring elements of the lateral pattern. Hence, the detailed information on the longitudinal and the transverse magnetization fluctuations considerably extends the information achievable by photon or electron-based imaging techniques.

In the present study the magnetization distribution in a stripe array with an induced uniaxial magnetic shape anisotropy is followed as a function of the magnetic field. The magnetization reversal is characterized by multi-domain states and correlations between the individual stripes. We present results from two preferential orientations of the magnetic field with respect to the direction of the magnetic stripes by combining the benefits of magneto-optic Kerr-effect (MOKE) and Kerr microscopy (KM) with results from PNR. While KM provides direct space images of magnetic domains, PNR probes both the parallel and the perpendicular components of the magnetization distribution in the Fourier space.

The sample studied is a $20 \times 10\,\mathrm{mm}^2$ polycrystalline magnetic stripe array consisting of stripes with a layer stack of 3 nm V, 76 nm $Co_{0.7}Fe_{0.3}$ and 3 nm of Al for protection, prepared by DC magnetron sputtering on a $Al_2O_3(1\,\bar{1}\,0\,2)$ substrate with a 5 nm thick Ta buffer layer. After depositing the Ta buffer layer, the sample was spin-coated with Novolak photoresist, which was exposed by 442 nm light in a scanning laser lithography setup and developed afterwards. Onto the patterned photoresist the Al/CoFe/V layer stack was deposited. Finally, the photoresist was removed via lift-off. The described procedure resulted in $Co_{0.7}Fe_{0.3}$ stripes of 2.4 μm width and a grating parameter of $d = 3\,\mu\mathrm{m}$ as can be seen from the AFM picture in Fig. 1.

Polarized neutron reflectivity experiments were performed at the ADAM reflectometer of the Institute Laue–Langevin in Grenoble, France [7]. For the measurements we used a fixed neutron wavelength of 0.441 nm. For field-dependent measurements, an electromagnet was installed with a field direction perpendicular to the scattering plane and parallel to the incident neutron polarization axis. We were also able to rotate our sample around its surface normal in order to measure at different angles χ between the applied field $\mathbf{H}$ and the anisotropy axis. As schematically shown in Fig. 2, the magnetic induction vector $\mathbf{B} = \mu_0(\mathbf{H} + 4\pi\mathbf{M})$, with $\mathbf{M}$ being the magnetization vector of the sample, is displayed within the sample surface plane perpendicular to the scattering vector $\mathbf{q}$. The monochromatic polarized neutron beam hits the sample at an incident angle α_i. Reflected neutrons exit the sample under a final angle α_f and their spin state can be analyzed. In the experiment two non-spin-flip (NSF) reflectivities R^{++} and R^{--} and two spin-flip (SF) reflectivities R^{+-} and R^{-+}, with + for 'up'-neutrons and − for 'down'-neutrons have been measured.

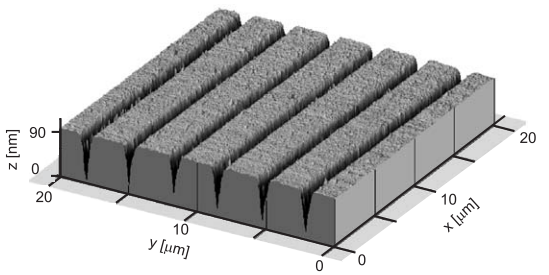

Fig. 1. Surface topography of an array of $Co_{0.7}Fe_{0.3}$ stripes obtained with an atomic force microscope shown in a three-dimensional surface view. The displayed area is $20 \times 20\,\mu\mathrm{m}^2$.

Additional to the specular reflectivity, Bragg reflections from the lateral period appear from the patterned sample. The reciprocal lattice of a stripe array is a linear dot pattern. With the orientation of the stripes parallel to the y-axis, as shown in Fig. 2, Bragg reflections occur along the x-axis. Rotating the stripes causes a rotation of the reciprocal lattice points from the x-axis to the x–y plane. Due to a poor resolution in the wave vector transfer projection q_y, compared to a high resolution in the projection q_x, Bragg reflections still can be observed at $q_x \approx (2\pi/d)\cos\chi$, where n is an integer and d is the lattice spacing [8,9]. Information on domain states can be gained from the off-specular scattering regime. Results from those measurements using a position sensitive detector and also quantitative simulations on the intensity maps are shown in Ref. [10].

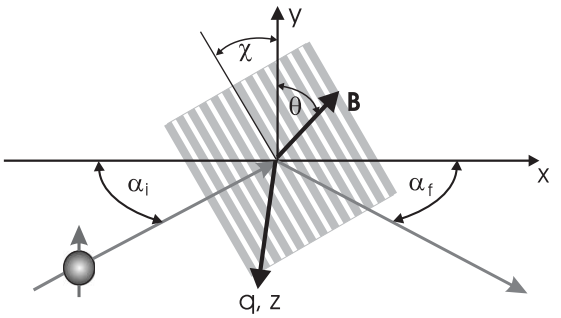

Fig. 2. Sketch of the scattering geometry for neutron reflectivity studies on patterned structures. The final state polarization analysis of the reflected neutrons is performed at the initial polarization directed either along, with, or opposite to the y-axis pointing along the external magnetic field. The latter is displayed within the film surface, but tilted with respect to the stripes so that the vector of the magnetic induction **B** makes the angle θ relative to the y-axis. For specular reflection the scattering vector **q** is parallel to the z-axis normal to the film surface, and α_i and α_f refer to the incident and exit angles of the neutrons to the sample surface. The sample rotation is expressed by the angle χ between the easy axis and the applied field.

With KM we observe ripple domain structures. The small-sized ripple domains appear already far below the coercive field H_c, close to remanence, and also show up above H_c. They can be observed for any angle of sample rotation and are presented in Fig. 3 for the easy-axis configuration $\chi = 0^\circ$ and for an angle $\chi = 75^\circ$, close to the hard axis, at fields $H_{ext} \approx H_c$. The contrast between neighboring domains is produced by magnetization directions, which are tilted away to the left and to the right relative to the net magnetization. By changing the magnetic field, the ripple domains do not change in size. At H_c, the nucleation of domains with the opposite average magnetization orientation sets in. The remagnetization process occurs by

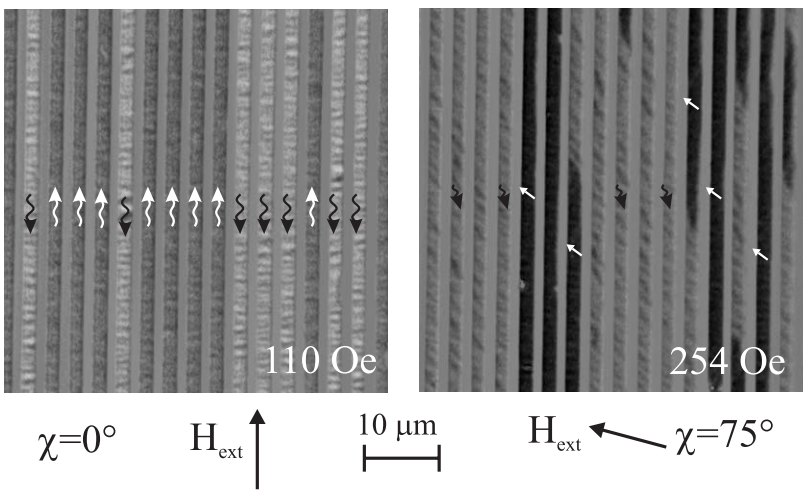

Fig. 3. KM images taken for two angles between magnetic field and sample: easy axis of $\chi = 0^\circ$ taken at $H_{ext} = 110$ Oe (left) and $\chi = 75^\circ$ taken at $H_{ext} = 254$ Oe (right). The plane of incidence results in a top-down magneto-optical sensitivity axis perpendicular to the stripes.

head-on-domain wall motion along stripes after nucleation of reverse domains. This motion is very fast and the magnetization in some stripes almost instantly alters its direction.

However, the reversal does not occur statistically independent in different stripes, but rather comprises several neighboring stripes. This was inferred for the easy axis $\chi = 0^\circ$ from additional KM studies (not shown here), using a lower resolution. In the Kerr image for $\chi = 75^\circ$ many domain walls are observed cutting the stripes into parts with opposite mean magnetization, in contrast to the rapid process at $\chi = 0^\circ$, where no head-on-domain walls were captured in the KM images. This observation for $\chi = 75^\circ$ is a result of the field alignment close to the effective hard-axis direction, favoring the generation of 'meta-domains' which are not limited to individual stripes and are shown in Fig. 4 taken with a low resolution.

We conclude that ripple domains and correlations in the multi-domain ensemble play an essential role in the reversal process of the laterally patterned film. Ripple domains are well known from thin films. They are induced by irregular anisotropies connected with the polycrystalline structure of the film [11]. We observed ripple domains, which also occur in the continuous film. In patterned films, ripple domains can be avoided if the shape anisotropy is large enough as was observed for 1.2 μm wide stripes [3]. But in the present case of 2.4 μm wide stripes this is not the case and ripple domains are abundant.

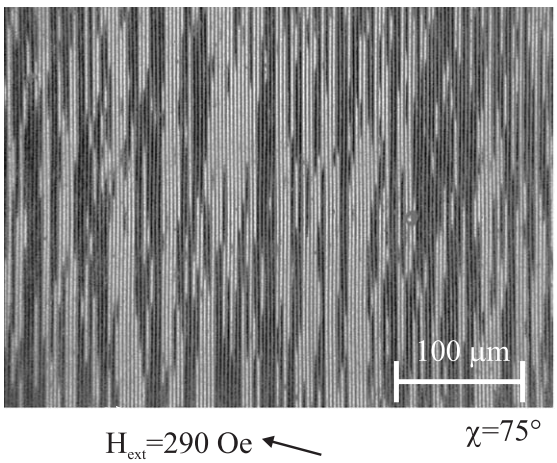

Fig. 4. KM image taken at $\chi = 75^\circ$ and $H_{ext} = 290$ Oe with a low resolution. The plane of incidence results in a top-down magneto-optical sensitivity axis perpendicular to the stripes.

The KM images in Figs. 3 and 4 already provide a good qualitative overview on the general features of the magnetization arrangement in the stripes and on the size distribution of the domains, ranging from several hundreds of nm to 1 μm in the parallel direction. However, they can hardly be used to obtain more quantitative information on the magnetization distribution at remanence and at higher fields. Neutron data provide the missing information by modeling the experimental results, implementing the information from the direct space KM images in Fig. 3 and from MOKE measurements as for subsequent evaluation of the PNR data.

We have taken reflectivity data with spin analysis of the exit beam at two angles of sample rotation $\chi = 0^\circ$ and 75°, providing two nonspin-flip (NSF), R^{++} and R^{--}, and two spin-flip (SF), R^{+-} and R^{-+}, reflectivities. As shown in Figs. 5(a) and (c), in saturation we observe the typical ferromagnetic splitting between R^{++} and R^{--} and almost no intensity for the SF reflectivities, $R^{+-} \approx R^{-+} \approx 0$. For $\chi = 0^\circ$ (Fig. 5(a)), in the range $0 \leqslant H \leqslant H_c$, the splitting between R^{++} and R^{--} is lowered and SF occurs, which is not expected for a typical easy-axis behavior. For $\chi = 75^\circ$ (Fig. 5(c)), the splitting between R^{++} and R^{--} gradually decreases and reaches zero for $H = H_c$, whereas the SF intensity increases towards its maximum at $H = H_c$. This behavior is typical for any orientation close to the hard axis. The SF intensities clearly indicate that the mean magnetization averaged over the lateral coherence range is not collinear with the applied field and has components perpendicular to the stripes.

The domain state of the stripes can be seen in the polarized reflectivity data by two main effects: first, for $\chi = 0^\circ$, the intensity of the specular and Bragg reflections is lowered, and secondly, the multi-domain state causes an asymmetric off-specular diffuse scattering, which is present at α_i and/or α_f close to the critical angles for total reflection [10]. Off-specular magnetic scattering occurs only when the domains are smaller than

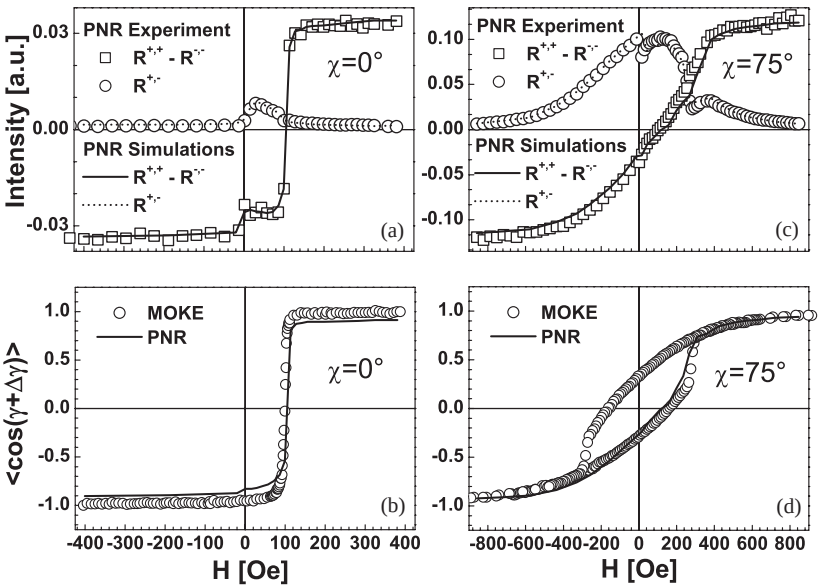

Fig. 5. Polarized neutron reflectivity measurements for sample rotation angles $\chi = 0^\circ$ (left column) and $\chi = 75^\circ$ (right column) (a) and (c). Field dependence of the NSF and SF reflectivities is compared to simulations (see text). Plotted is the difference of the NSF reflectivities $R^{++} - R^{--}$ (measurements: open squares, simulation: solid line), and the SF reflectivities $R^{+-} = R^{-+}$ (measurements: open circles, simulation: solid line); (b) and (d) field dependence of the mean projection of the normalized magnetization onto the easy axis as determined from MOKE (circles) and PNR (line) data.

the neutron coherence volume and when their magnetization vectors deviate from the mean magnetization direction within this coherence volume. The longitudinal coherence length projection (parallel to the neutron beam) is estimated to be more than 100 μm, while the transverse coherence length is only a few nm due to the focusing condition of the monochromater. The coherence volume, embracing a number of stripes and, consequently, a number of ripple domains in the lateral direction at $\chi = 0^\circ$, is sketched in Fig. 6. The scattering signal arising from different parts of the sample separated by distances greater than the coherence length should be accounted as statistically independent. Therefore, all interference effects from far separated areas are greatly cancelled out. On the contrary, within the coherence range constructive interference of scattering from periodic elements leads to a dramatic enhancement of scattering into distinguished directions, resulting in Bragg diffraction and specular reflection. The latter is, in fact, diffraction of the zero order.

In view of this it is pertinent to introduce the mean magnetization which is the average taken over ripple domains within the coherence area. This mean magnetization contributes to specular and Bragg reflections accounted by incoherently adding intensities from the different coherence areas. Note, that the mean magnetization may not coincide with the net magnetization averaged over a larger fraction of the sample and measured, for instance, via MOKE. While the net magnetization has a certain angle to the stripes, the mean magnetization is expected to deviate locally and show a large transverse and longitudinal distribution, as will be discussed in the following.

The model calculations are based on the domain state model sketched in Fig. 6 and have been accomplished using the distorted wave Born approximation (DWBA) [12]. The magnetization vectors within the domains, indicated by arrows, are tilted at angles $\gamma \pm \Delta\gamma$ with respect to the net magnetization directed along the stripe axis. The mean magnetization direction, denoted by the dashed arrows in Fig. 6, is $\gamma_{\mathrm{coh}} = \langle \gamma \pm \Delta\gamma \rangle_{\mathrm{coh}} \neq 0$.

Next, we consider the projection of the mean magnetization parallel and perpendicular to the net magnetization. This is especially important for the easy-axis configuration at $\chi = 0°$. Because of fluctuations of $\Delta\gamma$, the mean value is given by $\langle\cos(\gamma \pm \Delta\gamma)\rangle_{\mathrm{coh}} = c_\Delta c_\gamma \leqslant c_\gamma$, where $c_\gamma = \langle\cos\gamma\rangle_{\mathrm{coh}}$, $c_\Delta = \langle\cos\Delta\gamma\rangle_{\mathrm{coh}} \leqslant 1$, at $\langle\sin\Delta\gamma\rangle_{\mathrm{coh}} = 0$. At the same time the mean perpendicular magnetization component averaged over the coherence area, $\langle\sin(\gamma \pm \Delta\gamma)\rangle_{\mathrm{coh}} = c_\Delta\langle\sin\gamma\rangle \neq 0$, does not vanish even for the easy-axis configuration. It vanishes, however, for the easy-axis configuration after averaging over the whole sample. This is not the case for $s_\gamma^2 = \langle\sin^2\gamma\rangle \neq 0$, which causes SF specular reflection.

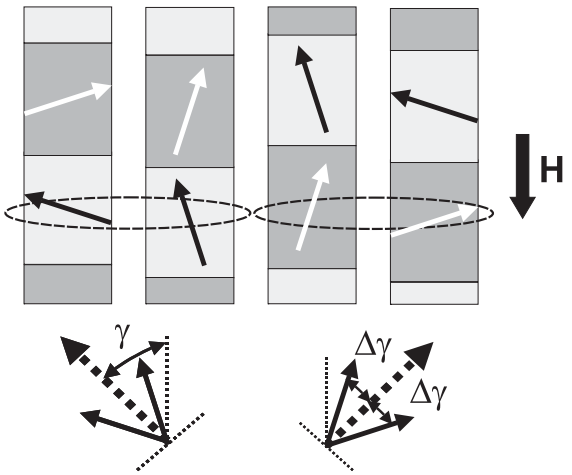

Fig. 6. Sketch for the model used in simulations for $\chi = 0°$. The dark and light gray shaded stripes represent the magnetic stripes with the ripple domains. The arrows indicate magnetization vectors within domains of individual stripes. The dashed line marks the neutron coherence volume, over which the average of the magnetization fluctuations are taken. For simplicity only two stripes within the coherence range are drawn, the actual size being much bigger. In the lower part of the figure the dashed arrows indicate the mean magnetization direction averaged over a coherence volume. γ is the angle of the mean magnetization vector with respect to the stripe orientation. $\Delta\gamma$ is the transverse fluctuation about the mean value. For further details see text.

The complete set of reflectivities, R^{++}, R^{--}, R^{+-}, R^{-+}, was fitted by varying three parameters, c_Δ, c_γ and s_γ^2, under the constrain $\langle\cos\gamma\rangle^2 \leqslant \langle\cos^2\gamma\rangle = 1 - s_\gamma^2$. In Figs. 5(a) and (c), the solid lines reproduce the simulations and the symbols are the experimental data points. Figs. 5(b) and (d) compare the mean value $\langle\cos(\gamma \pm \Delta\gamma)\rangle$ from MOKE measurements (solid line) with those deduced from PNR by the product $c_\Delta c_\gamma$. The fluctuations for the nearly hard-axis configuration at $\chi = 75°$ due to the ripple domains are only small deviations 'on top' of the already rotated magnetization compared to the direction of the applied field. For this direction, the effect of the ripples can hardly be separated in the specular reflectivity data. It can, however be seen from polarized intensity maps, which show strongly asymmetric off-specular scattering. As an example we show in Fig. 7 polarized neutron maps taken at

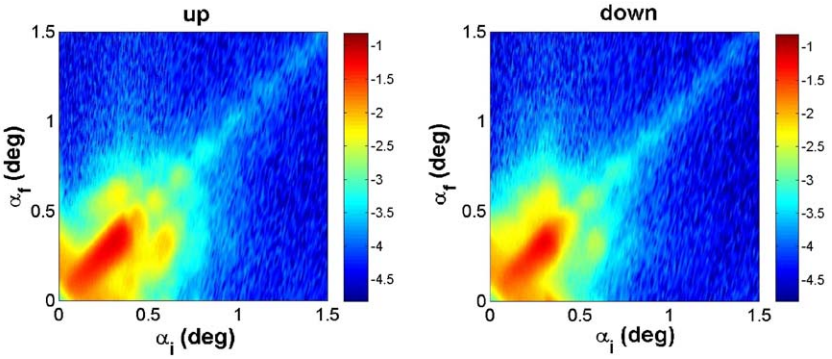

Fig. 7. Experimental maps of the polarized neutron intensity on a logarithmic scale from a periodic stripe array measured at a magnetic field of 310 Oe and plotted as a function of the angles of incidence α_i, and the scattering angles α_f. The left intensity map was measured with spin-up and the right with spin-down neutrons.

310 Oe, close to the coercive field. Due to the 'meta domains' (Fig. 4) occurring at H_c and having diameters of more than 100 μm, which is in the range of the coherence length, the intensity of the off-specular scattering is very high, comparable to the intensity of the specular reflectivity.

In the easy-axis configuration at $\chi = 0^\circ$, ripples play an essential role for the re-magnetization process. The occurrence of ripple domains gives rise to a transverse magnetization component and also is responsible for correlations between the magnetization in individual stripes [10]. Correlations due to dipole–dipole interactions are assumed to occur over distances of about 20 μm for the easy-axis configuration. For $\chi = 75^\circ$ correlations occur on a much larger scale covering the complete longitudinal coherence length.

In summary, we have shown that polarized specular and off-specular neutron scattering provides a detailed picture of the mean domain magnetization vectors in a magnetic stripe array, including longitudinal and transverse fluctuations about the mean magnetization and correlation effects between magnetic domains across different stripes. As a result of a quantitative analysis we have found that the domain magnetization vectors are strongly correlated not only parallel to the stripe direction, but also over a large perpendicular distance between them. This creates an inherent instability of the system with respect to the formation of large domains as observed during the magnetization reversal.

We thank V. Leiner, M. Wolff, A. Westphalen, K. Rott and H. Brückl for collaboration and fruitful discussions. We acknowledge funding by DFG, SFB 491 and by BMBF O3ZA6BC1.

References

[1] S.A. Wolf, D.D. Awschalom, R.A. Buhrman, J.M. Daughton, S. von Molnar, M.L. Roukes, A.Y. Chtchelkanova, D.M. Treger, Science 294 (2001) 1488.
[2] K. Temst, M.J. Van-Bael, V.V. Moshchalkov, Y. Bruynseraede, H. Fritzsche, R. Jonckheere, Appl. Phys. A 7 (2002) S1538.
[3] K. Theis-Bröhl, T. Schmitte, V. Leiner, H. Zabel, K. Rott, H. Brückl, J. McCord, Phys. Rev. B 67 (2003) 184415.
[4] N.D. Telling, S. Langridge, R.M. Dalgliesh, P.J. Grundy, V.M. Vishnyakov, J. Appl. Phys. 93 (2003) 7420.
[5] N. Ziegenhagen, U. Rücker, E. Kentzinger, R. Lehmann, A. van der Hart, B. Toperverg, Th. Brückel, Physica B 335 (2003) 50.
[6] W.-T. Lee, F. Klose, H.Q. Yin, B.P. Toperverg, Physica B 335 (2002) 77.
[7] A. Schreyer, R. Siebrecht, U. Englisch, U. Pietsch, H. Zabel, Physica B 248 (1998) 349.
[8] B.P. Toperverg, G.P. Felcher, V.V. Metlushko, V. Leiner, R. Siebrecht, O. Nikonov, Physica B 283 (2000) 9395.
[9] B. Dorner, A. Wildes, Langmuir 19 (2003) 7823.
[10] K. Theis-Bröhl, V. Leiner, A. Westphalen, H. Zabel, J. McCord, K. Rott, H. Brückl, B.P. Toperverg, Phys. Rev. Lett., submitted.
[11] A. Hubert, R. Schäfer, Magnetic Domains, Springer, Heidelberg, 1998.
[12] B.P. Toperverg, Physica B 297 (2001) 160;
B.P. Toperverg, Appl. Phys. A 74 (2002) S1560.